Meteoritics & Planetary Science 41, Nr 3, 391–405 (2006)
Abstract available online at http://meteoritics.org

Analysis and survival of amino acids in Martian regolith analogs

James R. C. GARRY[1*], Inge LOES TEN KATE[1, 2], Zita MARTINS[1], Per NØRNBERG[3], and Pascale EHRENFREUND[1]

[1]Astrobiology Laboratory, Leiden Institute of Chemistry, Leiden University, 2300 RA Leiden, The Netherlands
[2]Leiden Observatory, Leiden University, P.O. Box 9513, 2300 RA Leiden, The Netherlands
[3]Department of Earth Sciences, University of Århus, Ny Munkegade, DK-8000 Aarhus, Denmark
[*]Corresponding author. E-mail: j.garry@chem.leidenuniv.nl

(Received 24 August 2005; revision accepted 26 October 2005)

Abstract–We have investigated the native amino acid composition of two analogs of Martian soil, JSC Mars-1 and Salten Skov. A Mars simulation chamber has been built and used to expose samples of these analogs to temperature and lighting conditions similar to those found at low latitudes on the Martian surface. The effects of the simulated conditions have been examined using high-performance liquid chromatography (HPLC). Exposure to energetic ultraviolet (UV) light in vacuum appears to cause a modest increase in the concentration of certain amino acids within the materials, which is interpreted as resulting from the degradation of microorganisms. The influence of low temperatures shows that the accretion of condensed water on the soils leads to the destruction of amino acids, supporting the idea that reactive chemical processes involving H_2O are at work within the Martian soil. We discuss the influence of UV radiation, low temperatures, and gaseous CO_2 on the intrinsic amino acid composition of Martian soil analogs and describe, with the help of a simple model, how these studies fit within the framework of life detection on Mars and the practical tasks of choosing and using Martian regolith analogs in planetary research.

INTRODUCTION

Mars' current atmospheric pressure is too low to allow pure liquid water to persist at its surface—liquid water will freeze and evaporate. Data from orbiters and rovers (Haskin et al. 2005; Squyres et al. 2004) indicate that liquid water was present in significant amounts on Mars in the past, possibly allowing biologically important reactions to occur (Squyres 1984). The question of whether life arose on Mars has therefore been widely discussed in the planetary community since the conditions in its early history may have resembled those of the early Earth by having a dense atmosphere and persistent liquid water at its surface (McKay 1997). However, a combination of energetic UV radiation, the extreme dryness, and the presumed oxidizing nature of the soil make Mars' present surface an inhospitable place for terrestrial organisms. Organic matter carried by impacting meteorites appears to be affected by the same processes. The Viking Mars landers attempted to detect organic molecules in the upper surface three decades ago, but no evidence was found for organic matter that was not already present at low levels within the spacecraft's analysis equipment (Biemann et al. 1977). However, the lower detection limit of the Pyrolysis Release experiment of Viking would not have detected bacterial communities numbering in the millions per gram (Klein 1978). Thus, while many mechanisms have been proposed to explain the overall negative response of the Viking experiments, it is possible that organic matter may have been present, but at concentrations lower than could be detected by the equipment.

An international effort of solar system exploration will utilize several space missions to search for extinct or extant life on Mars during the next decade. In this context, it is vital to obtain knowledge about the survival of organic material exposed to Martian conditions. Laboratory simulations provide a convenient path to understand chemical reactions on the Martian surface, and studies have shown that there are a number of processes, both photochemical and photolytic, that reproduce aspects of the biological results of Viking, a summary of which can be found in Klein (1978). It is known that pure amino acids can be destroyed by exposure to UV light with a spectrum similar to that found at the surface of Mars and the rate of degradation is high relative to geological time scales (ten Kate et al. 2005; Stoker and Bullock 1997). Unshielded glycine and D-alanine molecules have half-lives of the order of 10^4 to 10^5 sec under noon-time conditions at

the Martian equator (ten Kate et al. 2005). More complex molecules are expected to be altered either by photolytic or photochemical pathways. Of particular interest is the possible role of water, either through the formation of gaseous oxidizing agents in the atmosphere or when chemisorbed into minerals or present as thin quasi-liquid films.

In this paper, we report data on the native amino acid content of Martian analogs using HPLC coupled with UV fluorescence detection. This technique is well suited to the analysis of complex mixtures of organic matter and by using this method we have quantified the native amino acid content of the Mars-1 material from Johnson Space Center (JSC) and a Danish soil (Salten Skov), both of which are internationally used Martian soil simulants. These materials were then exposed within a specially designed cryogen-cooled simulation chamber to temperature, UV lighting, and pressure that are similar to those on Mars. The composition and properties of the Martian soil analogs are discussed in the Regolith Analogs section, and the HPLC analyses are described in the Experiments and Methods section. Our experimental simulations are outlined in the Results section, with the results summarized in the Discussion section. We then discuss the implications of these Martian simulations in the context of future exploration efforts to detect organic molecules in the Martian subsurface.

REGOLITH ANALOGS

The two materials used in this study have different physical characteristics and mineralogy. It is not our intent to examine the broader view of how the degradation rate of organic matter varies with general properties of regoliths such as grain size or mineralogy. Instead, by using materials that are available to the planetary science community, we provide information about these particular soil analogs that can be used for disciplines ranging from planetary protection to material compatibility tests, among others. Pertinent characteristics of each analog are summarized briefly in the following sections.

JSC Mars-1

A Martian soil analog, hereafter referred to as Mars-1, is available to the research community from JSC. It is an ochre-colored mixture of weathered volcanic ash collected from the Pu'u Nene cinder cone, located in the saddle between Mauna Loa and Mauna Kea volcanoes on the island of Hawai'i (Allen et al. 1997). This soil approximates the composition, grain size, density, and magnetic properties of Martian soil and has been used in a number of Mars-oriented research studies that examine physical (Sternovsky et al. 2002) and biological processes (Kral et al. 2004). The elemental abundances of the Mars-1 material are broadly similar to those inferred from Viking surface studies, although the degree to which its mineralogy is comparable to that of Martian surface is not well known. Optical microscopic imaging of the powder shows irregular unweathered grains and computer analysis with the NIH Image software package of these images was used to find the distribution of grain cross-sections. From these data, an effective grain diameter distribution was calculated using the assumption that the grains were substantially spherical, and the resulting data are shown in Fig. 1.

The broad range of grain sizes in the Mars-1 material causes a significant degree of self-sorting. This leads to a segregation of the material based on grain size. Additionally, it is possible that different mineralogies are present in the largest and smallest fractions of the material. Thus, two sub-samples were prepared from the bulk supply of Mars-1: one made up of the larger grains, and one predominantly containing the smaller grains. This separation was achieved by gentle shaking of approximately 500 g of the original material in a polyethylene bag, and such action is intended to replicate the agitation that might occur in transit or in simple handling of the bulk material. No contamination-control documents were available for the two types of analog used, and it is therefore possible that they contained organic material, such as plasticizers, that had migrated from plastic scoops, bags, and similar handling tools. The extent to which such contamination might occur is limited, since the presented area of the regolith powders (>100 m^2 per kg) is far larger than the internal area (~500 cm^2) of the smallest bag used in these experiments.

Salten Skov

This dark red Danish soil, named after its source in the central Jutland region, is rich in precipitates of iron oxides and is excavated from an area of several hundred m^2. To date, this analog has had limited use in Martian simulation studies, with emphasis placed on its fine grain size and magnetic properties. A mineralogical study of this analog has been made (Nørnberg et al. 2004), but as yet the localized nature of the soil and its chemical nature are not well understood. The silt and clay size fraction (<63 μm) used in this experiment makes up 35.5% of the particles smaller than 2 mm. This fraction was separated from the total sample by dry sieving. It has a free iron content of 35.8%, of which nearly 90% is crystalline iron oxides (DCB/Oxalate extraction). Most of the grains with a diameter <63 μm consist of aggregates, which can be split into particles ~2 μm in size. The particle size of the <63 μm fraction was determined by laser diffraction and the particle size distribution is seen in Fig. 2, which shows two charts of the same data. The leftmost chart uses the same scale as was used to plot the Mars-1 grain size data in Fig. 1, and illustrates the complete absence of particles with diameters larger than 0.2 mm. The second chart in Fig. 2 shows the same data as the left-most chart, but plotted over one-tenth of the physical scale, showing that the Salten Skov material is composed predominantly of dust-sized particles.

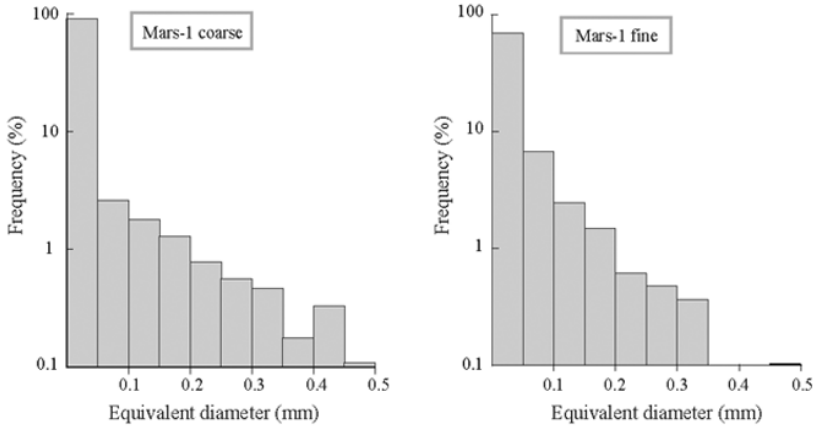

Fig. 1. The frequency distribution of grain diameters in two samples of the Mars-1 regolith.

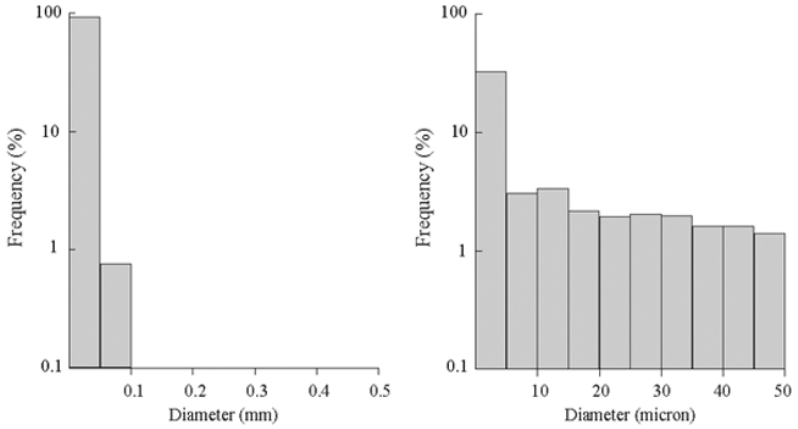

Fig. 2. The grain size distributions of the Salten Skov material used.

Control Material

The extent to which cross-contamination of the samples occurred within the irradiation chamber was monitored by the use of a third material. This control sample was a quantity of finely crushed Pyrex. It was expected that accidental transport of grains during the use of the chamber's pumping equipment, or sublimation and recondensation of the amino acids when in vacuum, might be observed by the detection of novel compounds in the Pyrex at the end of the experiment.

EXPERIMENTS AND METHODS

Samples

All of the samples were separately ground into powder in a glove box purged with argon gas and were stored in sterilized glass vials before being used in the experiments. An unused Pyrex test tube was crushed into powder and then heated to 500 °C for 3 hours for use as a reference blank, using the same process as for the samples.

Chemicals and Reagents

All tips and Eppendorf tubes used in this work were sterilized. All tools, glassware, and ceramics were sterilized by baking in aluminum foil at 500 °C for 3 hours. Amino acid standards were purchased from Sigma-Aldrich. AG 50W-X8 resin was acquired from Bio-Rad. Sodium hydroxide and hydrochloric acid (37%) were purchased from Boom, and ammonium hydroxide (28–30 wt%) was obtained from Acros Organics. *o*-Phthaldialdehyde (OPA), N-acetyl-L-cysteine (NAC), sodium acetate trihydrate, sodium borate decahydrate, as well as HPLC-grade water were bought from Sigma-Aldrich and methanol (absolute, HPLC-grade) was purchased from Biosolve Ltd.

Regolith Simulation Chamber

A stainless steel vessel was built that allowed up to seven sample cups to be cooled and simultaneously irradiated with UV light. The general form of the chamber is shown schematically in Fig. 3. A cylindrical block of brass held the

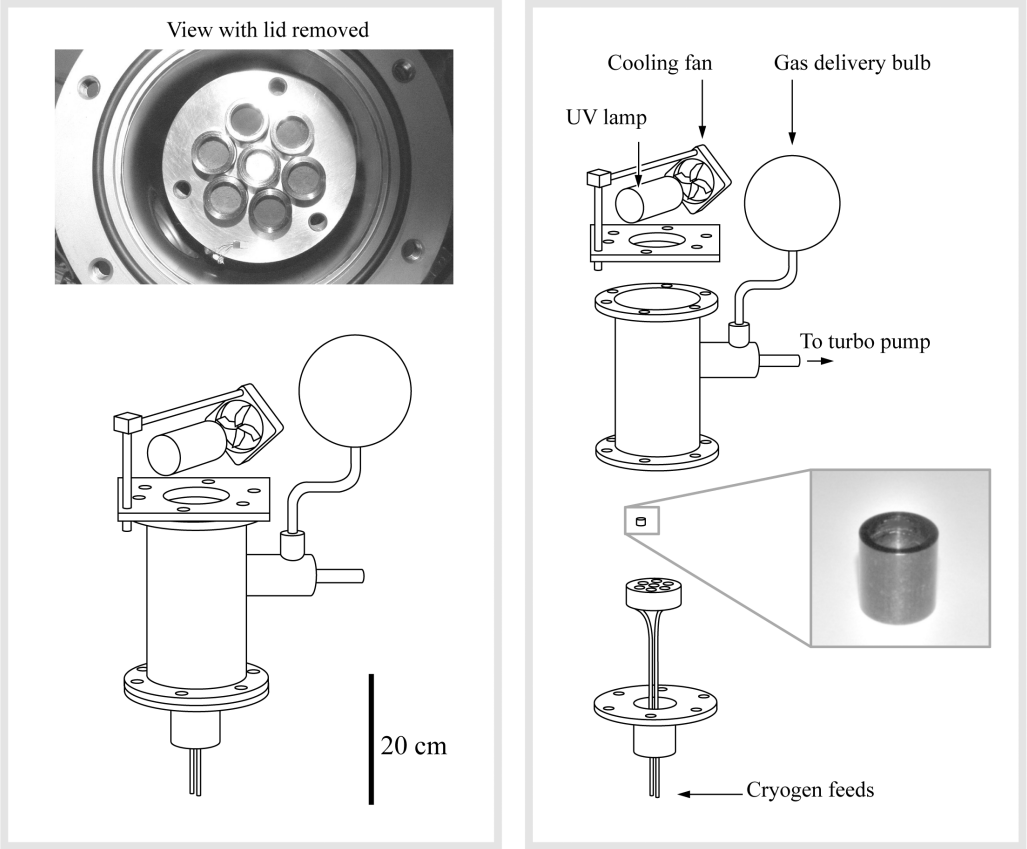

Fig. 3. The regolith exposure chamber, shown assembled in the lower left image and in its disassembled state in the right-hand image.

seven stainless steel sample cups in six recesses around its perimeter with one recess in the center. In this way all of the soil analog samples had the same distance (~105 mm) from the discharge region of an external deuterium discharge lamp and thus received illumination of the same intensity. The brass block was soldered to a coiled copper pipe that exited the chamber via a flange. A Dewar vessel holding pressurized liquid nitrogen was connected to this copper pipe, and a solenoid valve was used to modulate the cryogen flow so as to control the temperature of the brass block. The solenoid valve was controlled by a digital thermal controller wired to a platinum thermometer fixed to the sample holder block.

A turbo pump was used to evacuate the chamber and was backed by a two-stage rotary pump. No special precautions were taken to prevent oil back-contamination as the analysis performed on the samples is insensitive to the hydrocarbons present in pump lubricants.

Lighting System

The UV light was provided by a high-stability deuterium discharge lamp (Heraeus Noblelight, DX202). This lamp was held above the chamber's window inside an air-cooled shroud. A UV sensor (Solartech, model 8.0) was used to measure the intensity of the lamp's output in a narrow wavelength range (246 to 264 nm) and provided data traceable to a NIST standard source with an accuracy of around 10%. To gain information about the irradiance of the lamp outside of this spectral range a deuterium lamp (Bentham Instruments Ltd., model R48) with a known spectral profile was used to calibrate the response of a monochromator equipped with a photomultiplier tube (PMT), which gave an output precision of around 10 mV for values covering the PMT's full-scale output of 0 to 300 mV. This monochromator observed the deuterium lamp's output at wavelengths from 200 to 360 nm and the resulting irradiance data were scaled to match the power measured by the narrowband UV sensor. The resulting spectral profile is shown in Fig. 4, and the total flux of the lamp in the target plane was calculated to be 10^{14} photons cm^{-2} s^{-1}. The thick gray line shows unconfirmed data from the lamp's manufacturer and is for guidance only, as those wavelengths lie outside the monochromator grating's range. For comparison, the irradiance expected on the equatorial surface of Mars at local noon is shown as a solid line, as predicted by the model of Patel et al. (2002) for a low-dust atmosphere. If the lamp's output is integrated, 85% of the energy delivered by the lamp falls in the wavelength range of 190 to 325 nm,

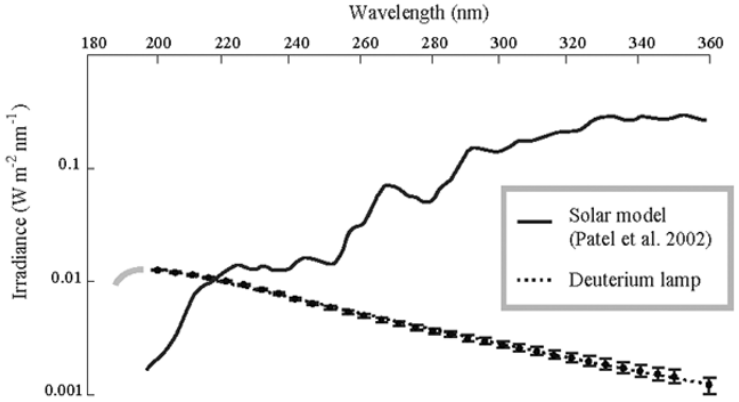

Fig. 4. The measured irradiance of the deuterium lamp in a plane 10 cm from the lamp's discharge point compared to the modeled irradiance at equatorial noon on Mars.

yielding an areal power in that range of 1 W m^{-2}. This evaluation criterion allows a comparison with the natural lighting found on Mars; for our experiments, the lamp yields a total intensity in the range of 190 to 325 nm that is one-tenth of the intensity at the Martian equator at local noon. It is also expected that the amino acid degradation results from the shorter rather than the longer wavelength light in that range. If the diurnal lighting variation is accounted for, one day of Martian illumination corresponds to 80 hours of lighting from the deuterium lamp.

Mars Simulation Experiments

Prior to the experiments, the stainless steel sample cups and the spoons used for filling the cups with the powdered analogs were cleaned with acetone and then with a solution of ethanol and demineralized water. After air drying, the cups were sterilized by baking at 300 °C for 3 hr. Six sample cups were filled with the chosen regolith analogs and one with the same amount of crushed Pyrex, serving as a control sample. The soil-containing cups were placed in the recesses around the perimeter of the brass sample holder, with the Pyrex control positioned in the center. The chamber was then evacuated to the operating pressure of around 1×10^{-5} mbar in the course of a few hours.

Four experiments were performed; in experiment I, samples were exposed for 24 hr to UV irradiation in vacuum (~1×10^{-5} mbar). These conditions were similar to those employed by ten Kate et al. (2005) and thus provide an immediate comparison for the effect of embedding amino acids in a regolith. An extended version of experiment I was performed, exposing fresh samples to 7 days of UV irradiation in vacuum (~1×10^{-5} mbar) and was named experiment II. Both of these experiments were conducted at room temperature (RT). A third experiment, illuminating new samples of the same materials for 7 days at a low temperature (210 K), was performed in a 7 mbar CO_2 atmosphere and is referred to as experiment III. In this last experiment, the turbo pump was shut off from the chamber and a glass vessel of known volume holding CO_2 (Praxair, 99.996% purity) at a known pressure was connected to the chamber. This last experiment was designed to permit water vapor to accrete at the surface of the samples. At the chosen temperature of 210 K, water ice has a smaller partial pressure than the ambient gas in the chamber and the vestigial amount of water outgassing from the stainless steel of the chamber would accrete onto the sample holders. By cooling the samples, and in doing so coating them with a thin water film, the work described in ten Kate et al. (2006) could be extended, in which the photolytic UV destruction rates of cold amino acid films were measured. In that work, cooling of the samples led to a reduction in the rate of photolysis (ten Kate et al. 2006) for glycine and in the Disucssion section the influence of water films on the degradation of organic matter adhered to real mineral surfaces will be examined.

The photolytic destruction of thin films of amino acids in vacuum has been described earlier by ten Kate et al. (2005), and so an additional experiment was conducted to verify that there were no unwanted influences arising from the use of the irradiation chamber. A silicon disc was coated with a sub-micron layer of glycine and placed in the regolith illumination chamber. The disc was then illuminated with the UV lamp in vacuum. In contrast to the first three experiments, which used HPLC analysis, the amount of glycine on the silicon disc was measured with a Fourier transform infrared (FTIR) spectrometer (Excalibur FTS-4000, BioRad, range 4000 to 500 cm^{-1}, 4 cm^{-1} resolution), in the manner described in ten Kate et al. (2005). Briefly, this consists of measuring the integrated area of specific regions in the infrared absorption spectrum of the silicon disc and its film both prior to and after irradiation in the regolith experiment chamber. Then, by assuming first-order reaction kinetics (Cottin et al. 2003) the destruction rate of the amino acid can be calculated from a linear fit through plots of the natural logarithms of the normalized integrated areas from the spectrum, both before and after irradiation.

HPLC Analysis

Each material was analyzed through use of an established procedure (Zhao and Bada 1995; Botta et al. 2002) for separating and analyzing amino acids in meteorite samples. This procedure requires that each sample was flame sealed in a test tube with 1 ml of water and boiled for 24 hours, at 100 °C in a heating block. One of two equal parts of the supernatants was then subjected to a 6 N HCl acid vapor hydrolysis for 3 hr, 150 °C. Both the hydrolyzed and the non-hydrolyzed extracts of the samples were desalted on a cation exchange resin, and the amino acids eluted from the resin with 5 ml of ammonium hydroxide. They were derivatized for 1 min or 15 min with OPA/NAC. The fluorescent OPA/NAC amino acid derivatives were separated by HPLC coupled with an UV fluorescence detector (Shimadzu, RF-10AXL). HPLC analysis was carried out in a C18 reverse phase (250 × 4.6 mm) Synergi 4μ Hydro-RP 80A column from Phenomenex, with UV fluorescence occurring by excitation at a wavelength of 340 nm and emission at 450 nm. The conditions for amino acid separations for the mobile phase at 25 °C were as follows; the flow rate was set at 1 ml min^{-1}, buffer A was 50 mM sodium acetate, containing 4% methanol (v/v), and buffer B was methanol. The gradient used was 0 to 4 min, 0% buffer B; 4 to 5 min, 0 to 20% buffer B; 5 to 10 min, 20% buffer B; 10 to 17 min, 20 to 30% buffer B; 17 to 27 min, 30 to 50% buffer B; 27 to 37 min, 60% buffer B; 37 to 49 min, 60% buffer B; 49 to 50 min, 60 to 0% buffer B; 50 to 60 min, 0% buffer B. Amino acids were identified by comparing their retention time with known standards. The amino acid abundances (part per billion by weight) in the soil samples were calculated by comparing the integrated peak area, corrected for the abundances in the blank Pyrex sample, with the integrated peak area of known amino acid standards.

RESULTS

Material Characterization

An investigation of the amino acid content in the two regolith analogs was made using HPLC. These materials were analyzed without any prior treatment, and were taken directly from the batches sent by their respective source institutes. Chromatograms for each of the materials used in this work are shown in Fig. 5.

The Mars-1 material was separated into two fractions, one having fine grains and one with coarser grains, as described earlier. Each of these fractions was sampled and analyzed three times by HPLC using two different derivatization periods. The average of the data from those three analyses are shown as rectangular columns in Fig. 6 and the minimum and maximum values of the data are shown by the upper and lower ends of the capped vertical bars.

The concentration by weight of the detected amino acids differs between the Mars-1 coarse and fine samples. Crudely, for a given amino acid, the concentration in the fine sample of Mars-1 is around one third greater than the concentration of that compound in the coarse sample. The near-uniformity of this relationship suggests that the organic content of the fine and coarse samples is a function of grain area. By contrast, no variation could be seen in the Salten Skov material in two portions of the material taken from the top and bottom of the bulk. This is probably because the material used had already been sieved to yield a narrow grain size distribution and thus rendered homogenous, as is seen by the tightly clustered values for the mean concentration for each amino acid in Fig. 7. An identical processing sequence was used for this material as was used for the Mars-1 regolith and the rectangular columns in Fig. 7 show the average of all the data per sample. Again, the capped vertical bars indicate the span of the data.

The Salten Skov material does not have the same amino acid distribution as the Mars-1 analog. Not only are the absolute concentrations of the detected amino acids higher by around a factor of 2 than in the Mars-1 regolith, but the Salten Skov material is richer in L-alanine and deficient in L-glutamic acid when compared to Mars-1. Despite their very different origins there are, however, common features in the amino acid make-up of the two soils that suggests that both Salten Skov and Mars-1 might have experienced a common contamination process, such as manual handling when they were collected. The ratio of L-valine/L-leucine in human sweat is around 2 (Hier et al. 1946), in broad agreement with the ratio seen in both the Mars-1 and Salten Skov materials. If contamination from handling is neglected, amino acids may still arise in the Mars-1 soil as a result of abiotic processes in the production of fresh volcanic ash (Markhinin and Podkletnov 1977) and the excavation site on Hawai'i will in any case be exposed to aerosol-carried contaminants. The material excavated at Salten Skov has probably not experienced aeolian deposition, but will have had groundwater and readily soluble amino acids from bacterial metabolism and decay percolating through it.

Mars Simulations

Four different experiments were performed. In each experiment, two samples of the Mars-1 material and two samples of the Salten Skov soil were used to ensure higher accuracy. A Pyrex control sample was also exposed in the center of the sample holder during each experiment. The weights of the samples were measured with a laboratory top-pan balance (Mettler AT200) and are shown in Table 1. Care was taken to ensure that the cups were not tilted or struck to preserve the layer-like state of the powders within. The small quantities of material resulted in layers around 1 mm deep. For each experiment, the same material was held in two diametrically opposed sample cups, hence two values are shown for each of the Mars-1 and Salten Skov weights in Table 1.

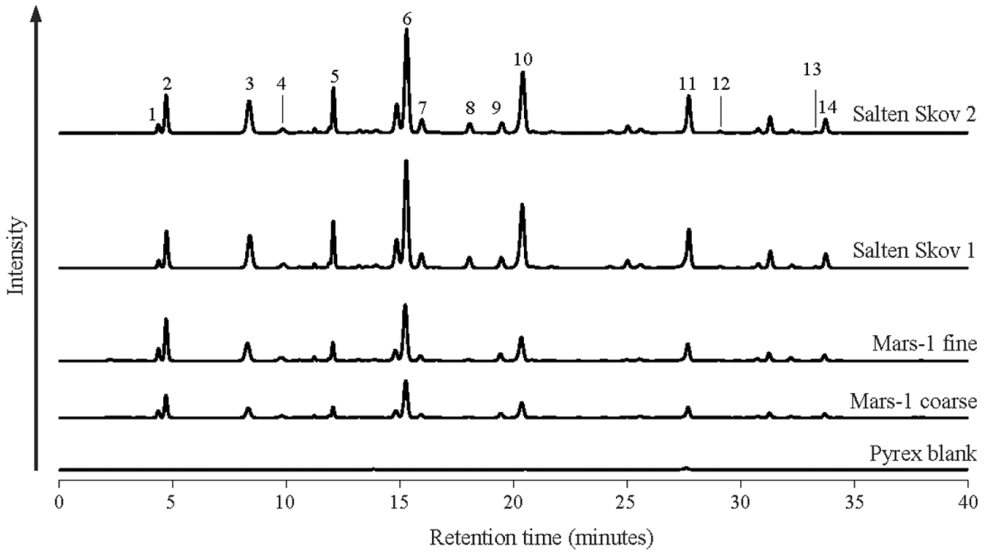

Fig. 5. The 0 to 40 minute region of the HPLC chromatograms for the un-irradiated materials. No peaks were detected outside this time period. OPA/NAC derivatization (1 minute) of amino acids in the Mars-1 coarse material, Mars-1 fine grain sample, Salten Skov samples and blank are shown. The peaks were identified as follows: 1: D-aspartic acid; 2: L-aspartic acid; 3: L-glutamic acid; 4: D-glutamic acid; 5: D, L-serine; 6: glycine; 7: β-alanine; 8: γ-amino-n-butyric acid (γ-ABA); 9: D-alanine; 10: L- alanine; 11: L-valine; 12: D-valine; 13: D-leucine; 14: L-leucine. Other peaks are discounted, due to lack of signal, or ambiguous interpretation for the standards used.

The conditions employed in the three experiments involving the irradiation of soils have been described in the Experiments and Methods section. Before the data from those experiments are shown, the results from the fourth experiment are discussed. As described in Experiments and Methods, a fourth test was performed to confirm that this particular experimental set-up could reproduce the degradation phenomena seen in earlier work using other equipment. A thin film of glycine was prepared in the manner described by ten Kate et al. (2005), placed in the regolith irradiation chamber, and exposed to the UV lamp under a pressure of 10^{-6} mbar. The disc and its glycine coating were studied by FTIR prior to and after irradiation. From these data points the destruction rate for a thin film of glycine was found to be $2.6 \pm 5 \times 10^{-6}$ molecules s^{-1}, which is approximately a factor of 2 larger than the figure calculated by ten Kate et al. (2005). This small difference can be attributed to the lack of data as the fixed arrangement of the samples in the chamber did not allow in situ measurements to be made of the film's IR transmission spectrum. In contrast, the equipment used by ten Kate et al. (2005) allowed a dozen or so transmission spectra to be recorded during the film's breakdown.

In Tables 2, 3, and 4 the amino acid concentrations of the different analogs are shown for the first three experiments performed. The amino acid concentration by weight of each material, shown in the columns labeled "Conc.," is the average of data from the two samples of that analog present in the chamber. The concentration shown for each of the three materials is an average of six HPLC measurements. The difference between the maximum and minimum values for the six concentration values for an amino acid in each material is tabulated in the columns headed "Span." Those values reflect the scatter in the concentration data and given the complexity of the extraction and subsequent HPLC processes should not be interpreted as an error in the sense of a random process occurring over many repeated identical trials.

Data for experiment I, consisting of exposure to UV light and vacuum at room temperature for one day, are shown in Table 2. In Table 3, the data from experiment II, involving exposure to UV light and vacuum at room temperature for seven days, are shown. Finally, in Table 4, the data from experiment III are listed, in which the samples were irradiated and cooled to 210 K in a CO_2 atmosphere.

For clarity, the shifts between the concentration of amino acids in the unirradiated samples and the concentrations in the soils in each of the three experiments (I, II, and II) are shown in Figs. 8 and 9 for the Mars-1 fine-grain analog and the Salten Skov material, respectively. The JSC Mars-1 coarse fraction data are not plotted, as they substantially follow the trends of the finer fraction.

DISCUSSION

The data shown in Figs. 8 and 9 appear to show three trends. First, there is an apparent increase in the concentrations of certain amino acids as a result of exposure to vacuum and UV light. For the Salten Skov material, the largest relative increase is seen for L-aspartic acid, which more than doubles in concentration when compared to its unirradiated concentration. The Mars-1 fine fraction displays broadly similar but smaller relative changes, with L-leucine doubling in concentration and the remainder rising in

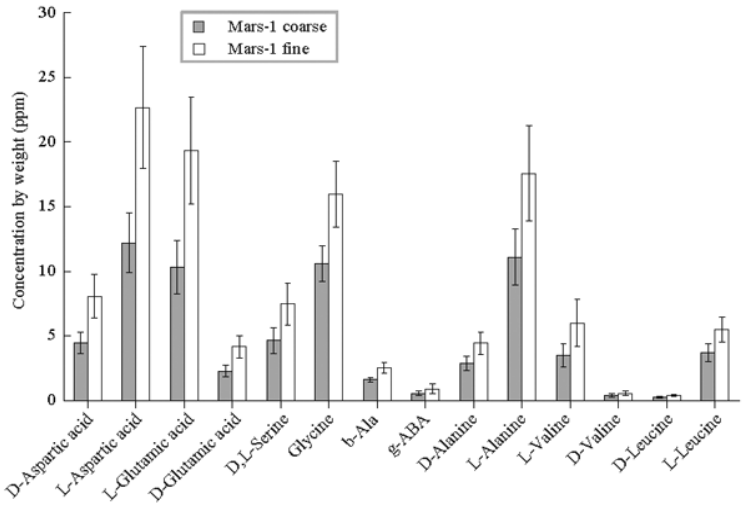

Fig. 6. Average absolute blank-corrected amino acid concentration in the unirradiated samples of coarse and fine-grained fractions of Mars-1.

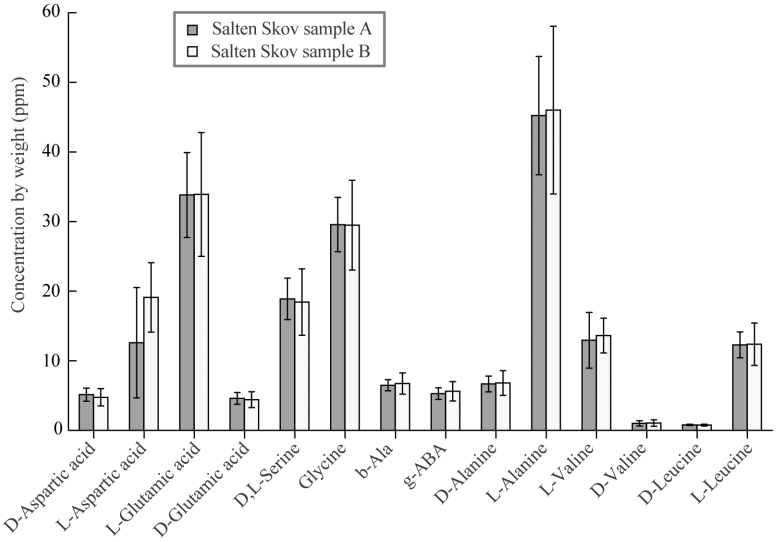

Fig. 7. Average absolute blank-corrected amino acid concentration in two samples of unirradiated Salten Skov material.

concentration by a lesser amount upon exposure to vacuum and UV light. No obvious sources of contamination were identified, and the same procedures were followed for analysis of pre-irradiated and post-irradiated samples, which ordinarily yielded values that were repeatable to a few ppm (Fig. 6). Second, the concentrations of the detected amino acids in the regolith samples do not change significantly when the UV exposure duration is changed from 1 day to 7 days, indicating that the process causing the rise in amino acid concentrations is rapid. Third, in experiment III the concentrations of the measured amino acid after irradiation were uniformly lower than the concentrations of the amino acids recorded at the end of experiment II. This change is most pronounced in the Mars-1 data, which show a reduction in the amino acid concentration to levels broadly below that of the unirradiated samples. Experiments by ten Kate et al. (2006) demonstrates that cooling pure films of amino acids to 210 K slows down their rate of degradation by a factor of 7 or so when they are exposed to a UV source. The lamp used in that work is the same model as used in the fourth experiment presented here, and it is therefore apparent that photolytic degradation cannot explain the absolute reduction in amino

Table 1. Showing the conditions and sample weights (mg) in each experiment.

	Experiment type		
Sample	I: 1 day UV, vacuum, ~300 K	II: 7 days UV, vacuum, ~300 K	III: 7 days UV, CO_2, 210 K
Pyrex blank	38.3	30.0	38.4
Mars-1 coarse	31.2, 31.3	30.3, 30.7	29.3, 30.2
Mars-1 fine	30.2, 29.8	30.1, 30.8	31.0, 33.2
Salten Skov A	35.5, 29.1	30.4. 33.1	29.6, 34.8

Table 2. Absolute blank-corrected amino acid average concentration (in ppb by weight) and data scatter from HPLC measurements in experiment I.

	Fine Mars-1		Coarse Mars-1		Salten Skov	
Amino acid	Conc.	Span	Conc.	Span	Conc.	Span
D-aspartic acid	10,375	1018	8939	1119	9521	1071
L-aspartic acid	24,164	2262	20,989	1502	35,404	4482
L-glutamic acid	18,499	1801	15,963	1483	43,769	4936
D-glutamic acid	5113	621	4390	761	6846	933
D,L-serine[a]	6931	1364	5930	897	23,037	2518
Glycine	20,764	2171	18,542	2577	44,047	5470
β-Ala	4685	393	4128	398	9997	1112
γ-ABA	1678	182	1373	200	6660	746
D-alanine	6469	750	5717	568	10,332	1646
L-alanine	17,368	2026	15,351	2038	54,002	6976
L-valine	3676	3326	3402	2804	16,393	6371
D-valine	600	451	524	285	1269	973
D-leucine	587	61	536	34	1518	304
L-leucine	5198	593	4597	379	16,294	2151

[a]Enantiomers could not be separated under the chromatographic conditions.

Table 3. Absolute blank-corrected amino acid concentration (in ppb by weight) and data scatter from HPLC measurements in experiment II.

	Fine Mars-1		Coarse Mars-1		Salten Skov	
Amino acid	Conc.	Span	Conc.	Span	Conc.	Span
D-aspartic acid	9947	1151	8315	710	7481	900
L-aspartic acid	27,335	3056	22,885	1921	38,393	4442
L-glutamic acid	21,299	2745	17,770	1541	45,993	5832
D-glutamic acid	4998	1219	4459	368	6108	1088
D,L-serine[a]	8777	1004	5757	3958	24,920	2563
Glycine	25,140	1299	24,024	1164	45,284	4968
β-Ala	5281	450	5320	428	10,281	1279
γ-ABA	2240	302	1506	285	6193	940
D-alanine	6293	680	5699	531	9116	1064
L-alanine	20,803	1502	18,000	1112	56,486	6817
L-valine	8007	4423	6142	3339	16,655	14,434
D-valine	336	228	376	177	915	485
D-leucine	436	66	397	87	959	144
L-leucine	5915	956	4784	786	17,641	2763

[a]Enantiomers could not be separated under the chromatographic conditions.

acid concentration that is seen in experiment III. A related experiment by ten Kate et al. (2006) shows that an ambient 7 mbar atmosphere of CO_2 at room temperature makes no measurable change to the UV-induced degradation rate of a thin amino acid film. That study argues that no significant quantities of reactive species are generated within the gas around the samples, as the degradation rate is essentially unchanged from that seen for amino acids in a hard vacuum. It is important to note that in experiment III, only the sample holder was cooled, not the whole chamber. Therefore, the gas within the chamber would have been substantially warmer than the 210 K of the brass sample holder and the soils. The difference between that study and the illumination of a soil is that in experiment III the organic matter is intimately connected to irregular mineral grains which will scatter and absorb infalling UV light rather than reflecting it. It is likely then that processes driven by UV quanta, such as the mobilization of electrons at a surface and the subsequent formation of trapped radicals, will proceed more effectively on UV-absorbing mineral surfaces coated with water than on a weakly absorbing or reflecting surface.

The apparent increase in amino acid concentrations as a result of exposure to vacuum and UV radiation is worthy of extended discussion. Neither the Mars-1 nor the Salten Skov samples were cleaned in any manner. Thus, it is likely that these materials contained organic contaminants from atmospheric aerosols, microbes from a variety of species, and bulk organic matter from the original excavation sites. Analysis of the JSC Mars-1 soil by Mendez et al. (2005) and Allen et al. (2000) showed the presence of fungi and

Table 4. Absolute blank-corrected amino acid concentration (in ppb by weight) and data scatter from HPLC measurements in experiment III.

	Fine Mars-1		Coarse Mars-1		Salten Skov	
Amino acid	Conc.	Span	Conc.	Span	Conc.	Span
D-aspartic acid	4345	784	6516	1621	5618	1057
L-aspartic acid	11552	2058	17583	4305	23828	4442
L-glutamic acid	9379	1614	14440	3552	31850	6001
D-glutamic acid	2175	445	3338	850	4403	1004
D,L-serine[a]	3644	479	5414	1390	15314	3516
Glycine	7095	1265	10900	2749	20618	3682
β-Ala	1751	307	2670	721	4744	884
γ-ABA	666	94	1699	436	3857	735
D-alanine	2392	425	3651	915	5617	1038
L-alanine	8104	1420	12383	3019	37181	7123
L-valine	6516	2460	7418	1435	19879	2540
D-valine	158	640	172	654	475	588
D-leucine	451	708	224	167	734	223
L-leucine	2245	1072	4000	964	12261	2262

[a]Enantiomers could not be separated under the chromatographic conditions.

culturable and non-culturable bacteria within it, and it is possible that the Salten Skov material could also be a host to bacterial or fungal spores. It is very likely that some of the apparent formation of amino acids such as L-glutamic, L-aspartic, L-alanine, and so on, indicates the degradation of cell walls and the lysis of living bacteria or bacterial spores present in the regoliths. Certainly, these amino acids are present in the cell wall proteins of common bacilli such as *E. coli*. A test of the degradation hypothesis (Howe et al. 1965) would require work perhaps involving some form of genetic or biomarker tracing. A similar rise is seen in the amino acid concentrations of the Mars-1 and Salten Skov material despite their different amino acid make-up in their unirradiated state. Therefore, it might be argued that such a common change is the result of a common biological process, such as spore degradation.

Model of Amino Acid Degradation Within a Regolith

The regolith analogs used in this work were exposed to the UV light generated by a deuterium lamp. No UV light with an intensity greater than 0.1 μW cm^{-2} in the range of 245 to 265 nm penetrated shallow (~1 mm thick) layers of Mars-1 or the Salten Skov material when illuminated with a UV intensity of 500 μW cm^{-2} from a xenon solar simulator. Thus, photolytic processes will only occur at the exposed surface of the regolith samples. If the powders are treated as spherical grains that are optimally packed, then the actual grain area that the radiation may strike is larger than the geometric cross-section of the sample cups. If the grains are assumed to be perfect absorbers, then only direct light from the lamp and radiation scattered from the sample cup walls can strike the regolith. If a vessel of radius R holds a powder of well-packed spheres with radius r, then only the upper hemispheres of the grains at the surface can be irradiated. Thus light penetrates only a distance r into the powder. The powdered sample has a known mass, m, and a bulk density ρ_{bulk}, and so the thickness of the sample is:

$$\frac{m}{\rho_{bulk}\pi R^2} \tag{1}$$

The sample holders have a cylindrical geometry, and so the total area of the sample varies linearly with sample thickness. Thus, the ratio, A, of the irradiated area at the surface to the total shadowed area is:

$$A = \frac{r}{\left(\frac{m}{\rho_{bulk}\pi R^2}\right)} \tag{2}$$

It will be assumed that all of the samples used have modal grain sizes of ~100 micron, as the difference between the coarse and fine Mars-1 materials appears to lie in the inclusion of large grains in the "coarse" sample rather than the exclusion of finer material. The weights of the materials used in each experiment were listed in table 1 and a nominal average bulk density, ρ_{bulk}, of 900 kg m^{-3} will be assumed; the bulk density of Mars-1 is around 900 kg m^{-3} for agitated samples (Allen et al. 1997). For the vessel (R = 5 mm) used to hold the powders, the fractional area, A, of a sample that receives direct radiation is of the order of 25% of the total surface area in the sample. Thus, if the regolith and any incumbent organic contamination with a photolytic characteristic lifetime of τ are exposed to a photolytically degrading process, then the concentration, C, of that organic matter remaining after time t is simply:

$$C = C_{(t=0)}\left[(1-A) + Ae^{-\left(\frac{t}{\tau}\right)}\right] \tag{3}$$

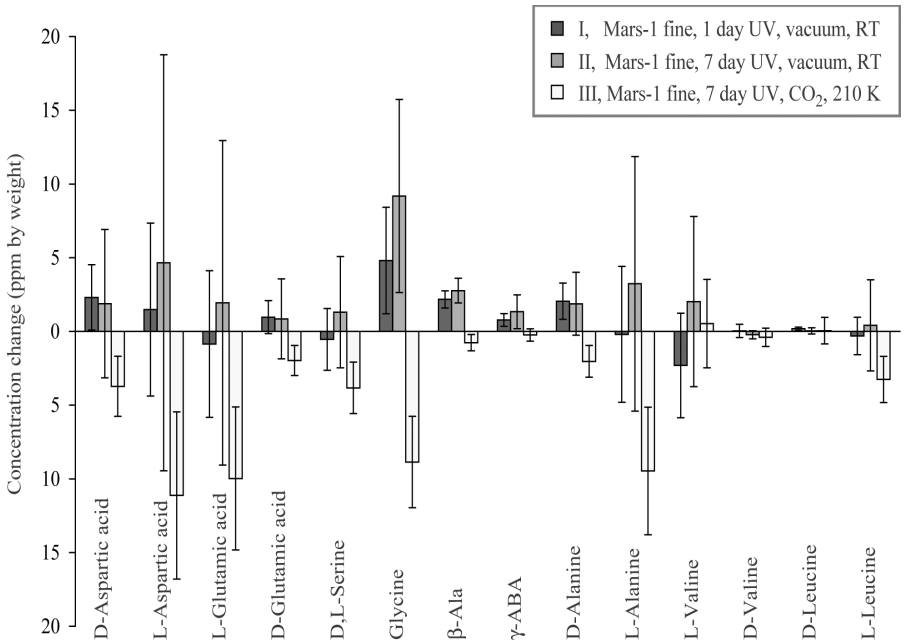

Fig. 8. The change in concentration in amino acids in the Mars-1 fine fraction resulting from experiments I, II, and III. An increase of certain amino acids can be observed after UV irradiation in vacuum at room temperature (RT). Enhanced destruction of D and L-aspartic acid, D and L-serine, L-glutamic, glycine, and L-alanine was observed in an experiment at 210 K and in a CO_2 atmosphere.

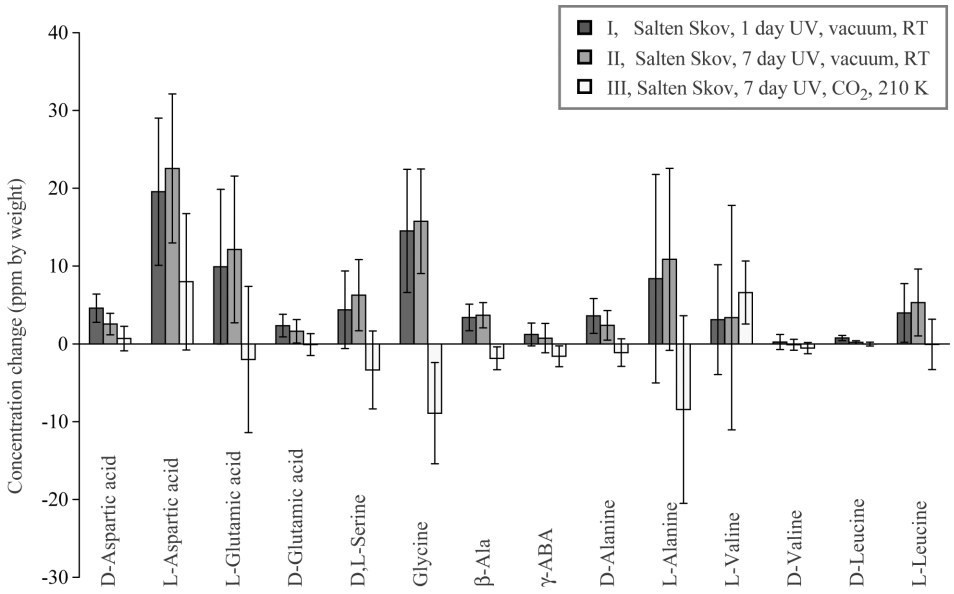

Fig. 9. The change in concentration in amino acids in the Salten Skov material resulting from experiments I, II, and III. An increase of certain amino acids was measured after UV irradiation in vacuum at room temperature. Enhanced destruction of glycine and L-alanine was observed in an experiment at 210 K and in a CO_2 atmosphere.

The photolytic degradation rates of glycine and D-alanine are known from earlier experiments (ten Kate et al. 2005) and so only these compounds will be discussed. D-alanine, with its half-life of 3 hr under Martian equatorial noon-time conditions, should have been completely removed from the upper *A* fraction of the analogs used in this work during one day. In that time the overall concentration glycine would have only been reduced by around 13%. Further irradiation for 6 days would not change the total amount of D-alanine in the regolith, as it will have been depleted from the region accessible to UV light, whereas the overall concentration of glycine would fall to ~75% of the original concentration. Given the accuracy and precision of the HPLC technique used, it is possible that this change would have been

detected. The absence, in experiment II, of a lowering of the amino acid concentrations suggests that either the grains stabilized surficial organic compounds against photolysis, or that the production of amino acids by the postulated breakdown of cell walls surpassed their photolytic removal.

Candidate Photochemical Processes

Several compounds and processes have been suggested as potential oxidizing agents that are presumed to operate at the Martian surface (Banin 2005; Zent and McKay 1994). It is worth examining some of these to assess whether the removal of amino acids in experiment III can be explained through the action of a reactive compound. For example, through photolysis water can form OH· radicals, which then can dimerize to hydrogen peroxide (H_2O_2), although other paths to its production are possible. The low thermal stability of H_2O_2 makes it a good candidate for the oxidation of matter at low temperatures, and on Mars it may be stable at significant depths within a regolith column (Bullock et al. 1994). The expected Martian equilibrium surface adsorbed concentrations for H_2O_2 are on the order of 250 nmoles cm^{-3}, based on a production rate of around 5×10^{10} cm^{-2} s^{-1} (Bullock et al. 1994). The formation of H_2O_2 is ultimately dependent on the concentration of water vapor in the atmosphere, and so it is possible to scale the production rate on Mars to the conditions present in the regolith illumination chamber. The chamber could be evacuated to a low pressure with the turbo pump. When the chamber was valved off from the pump's inlet, the pressure in the chamber rose over the course of a day to an equilibrium value of around 10^{-2} mbar. The source of this vapor is presumed to be water vapor outgassing from the regolith and from the chamber walls, this last source is expected in stainless steel vacuum systems that have been opened to ambient air. The partial pressure of water in Mars' atmosphere at the surface is believed to be around 10^{-3} mbar, and so a crude estimate for the production rate of H_2O_2 in the chamber from water photolysis can be made by comparing the optical path length of the chamber to the effective column height of Mars' atmosphere. By doing so, a formation rate of $\sim 10^6$ cm^{-2} s^{-1} is found, which results in a fractional areal coverage rate of one part in 10^8 per day for each regolith sample in the chamber. Changes in the amino acid concentrations over the course of one day would be undetectable with the HPLC method described in this work.

Water may also play a less direct role in forming oxidizing agents. It has been shown that the interaction of oxygen with UV irradiation (Oró and Holzer 1979) leads to the degradation of amino acids, but oxygen is a minor constituent of the Martian atmosphere. The presence of water frosts on mineral surfaces is pertinent as the exposure of thin water frosts on iron-bearing minerals to UV has been shown to cause the release of oxygen upon warming (Huguenin et al. 1979), arising from the formation of a condensed oxidizing agent at the mineral surface. Later experiments with feldspar by Yen et al. (2000) demonstrate that superoxide radicals such as O_2^- are formed through the combination of cold mineral surfaces (–30 °C), Mars-like UV lighting, free oxygen, and low concentrations of water. The quantum efficiency for this process has been estimated by Yen et al. (2000) as being 10^{-6} radicals $photon^{-1}$, who also predict a production rate of 10^7 cm^{-2} s^{-1}. It is appropriate to ask if these UV-generated radicals are therefore responsible for the degradation seen in experiment III. Our experiments with cooled mineral surfaces under UV irradiation were performed in an ambient gas with a mixing ratio of oxygen no greater than 50 ppm by volume according to the manufacturer's data sheets, this concentration is about 20 times smaller than that in the Martian troposphere. Thus, scaling for the lower illumination levels and oxygen content in the regolith chamber, approximately 10^4 radicals cm^{-2} s^{-1} would be expected to form on the surfaces of the regolith samples studied in this work. In the course of one day O_2^- radicals may have an areal coverage of 1 part in 10^{10} of the exposed regolith. The above calculations are based on the amount of gaseous oxygen in the CO_2 atmosphere of experiment III and neglects the potential for oxygen to be formed from the decomposition of adsorbed water by photolysis at the cold mineral surfaces of experiment III. It is therefore still possible that the amino acid degradation seen in experiment III is driven by oxidative attack from O_2^- radicals and perhaps other photochemical species, formed within the adsorbed water layers bound to the surfaces of the soil grains that are illuminated by energetic UV.

Water can also play a role as a mediating agent for the mobilization of acids generated through nitrogen and sulphur oxidation (Quinn et al. 2005). In the work presented here, neither of those compounds was present in the gas-phase at levels above a few ppb in any of the experiments, and so dry-acid deposition by aerosols is not expected. However, water adsorbed at the surface of a mineral can leach soluble species from the rock, leading to a situation in which Fe(II) ions generate OH· ions via the photo-Fenton reaction of H_2O_2 with the UV. This process is well studied on Earth (Southworth and Voelker 2003) and in Martian scenarios (Benner et al. 2000). Thus, a plausible pathway for the formation of a vigorous reactive species is present in experiment III involving the presence of water adsorbed onto mineral surfaces. In experiment III, the samples were cooled to 210 K in the presence of water with a partial pressure of around 10^{-2} mbar, around an order of magnitude higher than the partial pressure of water in the near-surface atmosphere of Mars (Schorghofer and Aharonson 2004). A theoretical model presented by Möhlmann (2004) indicates that a few monolayers of water would be ubiquitous on exposed Martian surfaces, with the total thickness fixed by the partial pressure of water. We therefore suggest that the samples within experiment III were coated with a quasi-liquid water

layer, permitting the generation of the OH· radicals to occur within that adsorbed water. The exact chemical path for its formation is not decidable from our data and several candidate pathways are available aside from those indicated in the Discussion section, such as the photo-Fenton reaction on iron-bearing minerals.

Comparison to the Martian Environment

The Martian surface experiences lighting spectra and material transport processes that are difficult to emulate in a laboratory. To first order, we assume that the spectrum of the light can be modeled with a fixed profile. In the apparatus used to illuminate the samples, the lamp produces an integrated power in the wavelength range of 190 to 325 nm that is around one-tenth of the intensity expected to occur in that band at noon in the equatorial regions of Mars. Furthermore, the surface of Mars is not a static environment and the action of wind, saltating grains, and sporadic meteorite impact act to till the regolith over different time scales. Thus, the uppermost UV-exposed regolith grains will be progressively mixed into the ground. If a grain is removed from the surface by some form of gardening in a time that is shorter than the organic matter's photolytic lifetime, then there will be no sharp boundary between the UV-cleansed upper surface and deeper layers.

A further relevant point concerns the use of constant temperatures for periods greater than one day: ~300 K in experiments I and II, and 210 K in experiment III. These conditions do not accurately reflect the equatorial diurnal temperature cycle seen on Mars, as the warming and cooling cycle experienced by the Martian surface throughout a full day is not simulated. This is an important factor as the reactivity of chemical species formed either through photochemical or photolytic pathways on the Martian surface will be influenced by the ambient temperature. The longevity of such species (H_2O_2, etc.) will also depend on the surface temperature, and their abundance will be influenced by the porosity of the regolith. It is possible that a balance will be struck between the rate at which a species may decompose during the day and the rate at which they may condense during the night. We do not mimic other processes occurring on Mars, such as burial by dust at sundown, that could lead to the preservation of oxidizing agents formed through interaction with water.

CONCLUSION

We have performed analyses of two Martian regolith simulants and have quantified their amino acid content. In doing so, we have obtained data that are useful to biological, chemical, and physical studies of analogs for Martian surface materials. If biological processes occurred on Mars in the past, they may have been exposed to climatic conditions different from those currently seen on that planet. The chemical signatures from these processes and the materials brought by meteorites throughout Mars' history are subject to a number of destructive processes that operate at different time scales and in the presence of different materials. We have studied the effect of an important process, UV radiation, on two soil analogs. Exposure of these materials to conditions of vacuum and energetic UV appears to generate higher concentrations of amino acids within the materials. This process is rapid and repeatable in all the samples used, with exposures of one day yielding results similar to those arising from seven days of irradiation. It should be noted that seven days of irradiation in the laboratory is equivalent to the light received during 2 full days on Mars. It is postulated that this in situ formation results from the degradation of extant biota within the soils, and the fingerprint of amino acids present is suggestive of the degradation of cell walls, as indicated in the Discussion section.

With the method used, photolysis of the amino acids present in the soils, or generated through cell destruction was not detected. The shallow samples permit a significant fraction (of order 30%) of the material to be irradiated, a value comparable to the precision of the HPLC process employed. Separately, we have demonstrated that a pure amino acid film can be degraded within the experimental chamber when the sample is lit by the UV lamp used in the experiments described here. The degradation rate from that measurement is in line with expectations from earlier work (ten Kate et al. 2005), and therefore photolytic degradation should occur in the regolith samples exposed to UV light, but other factors dominate the changes seen in the amino acid concentrations.

Cooling of the regolith samples to 210 K and simultaneous exposure to an atmosphere of carbon dioxide leads to the removal of amino acids when compared to unirradiated samples. It is probable that adsorbed water on the mineral surfaces is key to the generation of reactive species on the grains and the subsequent degradation of the amino acid content within the soil, as is discussed by Quinn (2005) and Zent and McKay (1994). While the details of the process are not visible from this work, it is worth noting that the amino acid degradation caused by cooling in the presence of background water is comparable in magnitude to the degradation expected by photolysis in the same period (see the Discussion section).

If the apparent formation of amino acids in regolith simulants is taken at face value, there are implications for the use of these and other analogs in future. The diverse nature of the planetary research community means that a single material cannot reasonably represent the wide range of physical and chemical properties that are pertinent to Martian science. A specific and timely concern is the nature of analogs that are appropriate for forthcoming missions that will engage in biological studies of in situ and returned Martian samples. For example, it is conceivable that materials used in

simulations of a sample return mission would, for the purpose of verifying the curation and dispersal procedures, be subject to the same planetary protection regulations as a real sample (Rummel 2001). As part of such a process, qualification samples with no detectable organic content would be needed. While the physical properties (such as grain size distribution and so on) of an analog can be controlled relatively easily, it is difficult to conceive of a process that would remove extant biota and their corpses from a regolith analog without changing the mineralogy of the material. Techniques employed in spacecraft sterilization processes such as heat-sterilization, irradiation with ionizing particles and quanta, and exposure to oxidizing gasses and plasmas, are unable to remove significant quantities of organic matter from a material. Thus, it would be desirable to establish a database of analogs for planetary regoliths which are separately designed for chemical, biological, and engineering studies. We have demonstrated that an analog, such as Mars-1, designed to be a spectral and physical match to a nominal average Martian soil is inappropriate for a life science study in its raw state.

Acknowledgments–JRCG is supported by grant MG058 from the SRON National Institute for Space Research, ILtK is supported by the BioScience Initiative of Leiden University, ZM is supported by Fundação para a Ciência e a Tecnologia (scholarship SFRH/BD/10518/2002), PE is supported by grant NWO-VI 016.023.003. We thank Zan Peeters for his help with the HPLC analyses and the clarity of this manuscript was improved by constructive comments from A. J. T. Jull and the reviewers M. Sephton and C. McKay. Oliver Botta is thanked for his insight into HPLC processing.

Editorial Handling—Dr. A. J. Timothy Jull

REFERENCES

Allen C. C., Griffin C., Steele A., Wainwright N., and Stansbery E. 2000. Microbial life in Martian regolith simulant JSC Mars-1 (abstract #1287). 31st Lunar and Planetary Science Conference. CD-ROM.

Allen C. C., Morris R. V. Lindstrom D. J., Lindstrom M. M., and Lockwood J. P. 1997. JSC Mars-1: Martian regolith simulant (abstract #1797). 28th Lunar and Planetary Science Conference. CD-ROM.

Banin A. 2005. The enigma of the Martian soil. *Science* 309:888–890.

Benner S. A., Devine K. G., Matveeva L. N., and Powell D. H. 2000. The missing organic molecules on Mars. *Proceedings of the National Academy of Sciences* 97:2425–2430.

Biemann K., Oró J., Toulmin P. III, Orgel L. E., Nier A. O., Anderson D. M., Simmonds P. G., Flory D., Diaz A. V., Rushneck D. R., Biller J. E., and Lafleur A. L. 1977. The search for organic substances and inorganic volatile compounds in the surface of Mars. *Journal of Geophysical Research* 82:4641–4658.

Botta O. and Bada J. L. 2002. Extraterrestrial organic compounds in meteorites. *Surveys in Geophysics* 23:411–467.

Bullock M. A., Stoker C. R., McKay C. P., and Zent A. P. 1994. A coupled soil-atmosphere model of H_2O_2 on Mars. *Icarus* 107: 142–154.

Cottin H., Moore M. H., and Bénilan Y. 2003. Photodestruction of relevant interstellar molecules in ice mixtures. *The Astrophysical Journal* 590:874–881.

Glavin D. P., Schubert M., Botta O., Kminek G., and Bada J. L. 2002. Detecting pyrolysis products from bacteria on Mars (abstract #1094). 33rd Lunar and Planetary Science Conference. CD-ROM.

Haskin L. A., Wang A., Jolliff B. L., McSween H. Y., Clark B. C., Des Marais D. J., McLennan S. M., Tosca N. J., Hurowitz J. A., Farmer J. D., Yen A., Squyres S. W., Arvidson R. E., Klingelhöfer G., Schröder C., de Souza P. A., Jr., Ming D. W., Gellert R., Zipfel J., Brückner J., Bell J. F. III, Herkenhoff K., Christensen P. R., Ruff S., Blaney D., Gorevan S., Cabrol N. A., Crumpler L., Grant J., and Soderblom L. 2005. Water alteration of rocks and soils on Mars at the Spirit rover site in Gusev crater. *Nature* 436:66–69.

Hier S. W., Cornbleet T., and Bergeim O. 1946. The amino acids of human sweat. *Journal of Biological Chemistry* 166:327–333.

Huguenin R. L., Miller K. J., and Harwood W. S. 1979. Frost-weathering on Mars: Experimental evidence for peroxide formation. *Journal of Molecular Evolution* 14:103–132.

Howe J. M., Featherstone W. R., Stadelman W. J, and Banwart G. J. 1965. Amino acid composition of certain bacterial cell-wall proteins. *Applied Microbiology* 13:650–652.

Klein H. P. 1978. The Viking biological experiments on Mars. *Icarus* 34:666–674.

Kral T. A., Bekkum C. R., and McKay C. P. 2004. Growth of methanogens on a Mars soil stimulant. *Origins of Life and Evolution of the Biosphere* 34:615–626.

Markhinin E. K. and Podkletnov N. E. 1977. The phenomenon of formation of prebiological compounds in volcanic processes. *Origins of Life and Evolution of the Biosphere* 8:225–35.

McKay C. P. 1997. The search for life on Mars. *Origins of Life and Evolution of the Biosphere* 27:263–289.

Mendez C., Garza E., Gulati P., Morris P. A., and Allen C. C. 2005. Isolation and identification of microorganisms in JSC Mars-1 simulant soil (abstract #2360). 36th Lunar and Planetary Science Conference. CD-ROM.

Möhlmann, D. 2004. Water in the upper Martian surface at mid- and low-latitudes: Presence, state, and consequences. *Icarus* 168: 318–323.

Nørnberg P., Schwertmann U., Stanjek H., Andersen T., and Gunnlaugsson H. P. 2004. Mineralogy of a burned soil compared with four anomalously red Quaternary deposits in Denmark. *Clay Minerals* 39:85–98.

Oró J. and Holzer G. 1979. The photolytic degradation and oxidation of organic compounds under simulated Martian conditions. *Journal of Molecular Evolution* 14:153–160.

Patel M. R., Zarnecki J. C., and Catling D. C. 2002. Ultraviolet radiation on the surface of Mars and the Beagle 2 UV sensor. *Planetary and Space Sciences* 50:915–927

Quinn R. C., Zent A. P., Ehrenfreund P., Taylor C. L., McKay C. P., Garry J. R. C., and Grunthaner F. J. 2005. Dry acid deposition and accumulation on the surface of Mars and in the Atacama desert, Chile (abstract #2282). 36th Lunar and Planetary Science Conference. CD-ROM.

Quinn R. C. 2005. Experimental characterization and in situ measurement of chemical processes in the Martian surface environment. Ph.D. thesis, University of Leiden, The Netherlands.

Rummel J. D. 2001. Planetary exploration in the time of astrobiology: Protecting against biological contamination. *Proceedings of the National Academy of Sciences* 98:2128–2131.

Schorghofer N. and Aharonson O. 2004. Stability and exchange of subsurface ice on Mars (abstract #1463). 35th Lunar and Planetary Science Conference. CD-ROM.

Southworth B. A. and Voelker B. M. 2003. Hydroxyl radical production via the photo-Fenton reaction in the presence of fulvic acid. *Environmental Science & Technology* 37:1130–1136.

Squyres S. W. 1984. The history of water on Mars. *Annual Reviews of Earth and Planetary Sciences* 12:83–106.

Squyres S. W., Grotzinger J. P., Arvidson R. E., Bell J. F. III, Calvin W., Christensen P. R., Clark B. C., Crisp J. A., Farrand W. H., Herkenhoff K. E., Johnson J. R., Klingelhöfer G., Knoll A. H., McLennan S. M., McSween H. Y., Jr., Morris R. V., Rice J. W., Jr., Rieder R., and Soderblom L. A. 2004. In situ evidence for an ancient aqueous environment at Meridiani Planum, Mars. *Science* 306:1709–1714.

Sternovsky Z., Robertson S., Sickafoose A., Colwell J., and Horányi M. 2002. Contact charging of lunar and Martian dust simulants. *Journal of Geophysical Research* 107:5105–5113.

Stoker C. R. and Bullock M.A. 1997. Organic degradation under simulated Martian conditions. *Journal of Geophysical Research* 102:10,881–10,888.

ten Kate I. L., Garry J. R. C., Peeters Z., Foing B., and Ehrenfreund P. 2006. The effects of Martian near surface atmospheric conditions on the photochemistry of amino acids. *Planetary and Space Science* 54:296–302.

ten Kate I. L., Garry J. R. C., Peeters Z., Quinn R., Foing B., and Ehrenfreund P. 2005. Amino acid photostability on the Martian surface. *Meteoritics & Planetary Science* 40:1185–1193.

Yen A. S., Kim S. S., Hecht M. H., Frant M. S., and Murray B. 2000. Evidence that the reactivity of the Martian soil is due to superoxide ions. *Science* 289:1909–1912.

Zent A. P. and McKay C. P. 1994. The chemical reactivity of the Martian soil and implications for future missions. *Icarus* 108: 146–157.

Zhao M. and Bada J. L. 1995. Determination of α-dialkylamino acids and their enantiomers in geological samples by high-performance liquid chromatography after derivatization with a chiral adduct of o-phthaldialdehyde. *Journal of Chromatography A* 690:55–63.